Amyloid probes based on Congo Red distinguish between fibrils comprising different peptides

Ted T Ashburn*†, Hogyu Han*, Brian F McGuinness‡ and Peter T Lansbury, Jr

Background: Amyloid plaques, which characterize degenerating tissue in Alzheimer's disease (brain) and type II diabetes (pancreas), were first visualized by staining with the dye Congo Red (CR). The ability of CR to recognize amyloid fibrils comprising diverse proteins suggests that the binding site includes an unidentified structural feature common to all amyloid fibrils. We set out to design and synthesize analogs of CR that could distinguish between fibrils comprising different peptides.

Results: Relative affinities of several CR analogs for two model amyloid fibrils were measured and compared to that of CR. Amyloid fibrils comprising peptides based on the critical carboxyl terminus of the Alzheimer's disease amyloid protein β1–42 (β34–42) and the critical region of the type II diabetes pancreatic amyloid protein, IAPP (IAPP20–29) were tested. The ratio of affinities of each individual CR analog for the two amyloid fibrils varied considerably. Complexation of certain metal ions (Cu(II), Zn(II), Ni(II), Cd(II)) by a CR analog did not abolish its affinity for amyloid but changed the affinity ratio significantly.

Conclusions: This study demonstrates that small organic and organometallic molecules are capable of detecting differences in amyloid fibril structure and/or amyloid protein sequence. Molecules of this type could have utility as neuropathological probes or imaging agents, since they are much easier to prepare and functionalize than antibodies and are specific for the fibrillar form of the amyloid proteins.

Address: Department of Chemistry, Massachusetts Institute of Technology, Cambridge, MA 02139, USA.

Present addresses: †Harvard Medical School, 260 Longwood Avenue, Boston, MA 02115, USA and ‡Pharmacopeia, Inc., Princeton, NJ, USA.

*The first two authors contributed equally to this work.

Correspondence: Peter T Lansbury, Jr
e-mail: ptljr@mit.edu

Key words: amylin, amyloid, Alzheimer's disease, Congo Red, type II diabetes

Received: **27 Feb 1996**
Revisions requested: **10 Mar 1996**
Revisions received: **20 Mar 1996**
Accepted: **22 Mar 1996**

Chemistry & Biology May 1996, **3**:351–358

 ISSN 1074-5521

Introduction

Alzheimer's disease (AD) was originally described, and is still diagnosed, based on the presence in the postmortem brain of proteinaceous deposits, known as amyloid plaques, that stain with the dye Congo Red (CR) [1,2]. Amyloid deposition is still the primary neuropathological criterion for the diagnosis of AD ([3]; the method described in this reference is one of many based on plaque density). Amyloid plaques contain a core of ordered fibrillar protein aggregates. In the case of AD, the predominant brain amyloid proteins are β1–42 and its carboxy-terminal truncated relative β1–40 [1] (Fig. 1). The carboxy-terminal sequence determines the rate of amyloid formation; β1–42 aggregates much more rapidly *in vitro* than β1–40 [4]. Monoclonal antibodies that distinguish β1–40 and β1–42 have been used to show that β1–42 is more prominent in the blood serum (Younkin, S.G., unpublished data) and in the postmortem brain [5] of patients with two classes of early-onset AD (caused by point mutations in a presenilin protein (chromosome 14) or in the amyloid precursor protein (chromosome 21)) relative to patients with late-onset disease. The peptide β34–42 has been studied as a model of the critical region of β1–42 amyloid [6–9]. Amyloid fibrils formed *in vitro* from β34–42 fibrils resemble naturally derived AD amyloid fibrils at the ultrastructural level, and the peptide fibrils produce a similar, yet more highly resolved, X-ray diffraction pattern [6]. The peptide fibrils *in vitro* and the native AD fibrils in brain sections both stain in a birefringent manner with Congo Red [6]. It is not yet possible, however, to determine if β34–42 and the carboxy-terminal region of the β1–42 amyloid fibrils are structurally identical [9,10].

Recently, a second protein component of the fibrillar plaque core has been described, called NAC (the non-Aβ component of AD amyloid) [11]. Although it is only a minor plaque component at the time of death (~10 % of total amyloid protein), NAC may trigger the pathogenic cascade by seeding amyloid formation by β1–40 [12]. Despite all of the convergent suggestive evidence, it is important to note that amyloidogenesis has not been proven to be a cause of AD neurodegeneration [1,13]. The major obstacle towards clarifying the relationship between amyloid deposition and neurodegeneration is that it is not currently possible to non-invasively monitor the deposition of brain amyloid. A long-term goal of the work described here is to develop new imaging agents that allow the comparison of the deposition of amyloid

Figure 1

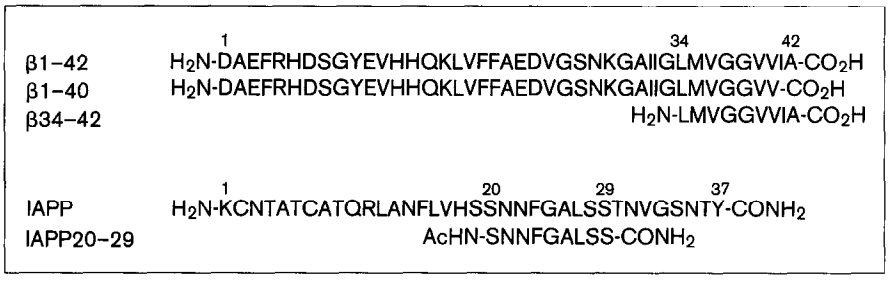

The sequences of β1–42, β1–40, IAPP and corresponding model peptides β34–42 and IAPP20–29.

over time (possibly distinguishing between different amyloid proteins) with the appearance of AD symptoms.

Other diseases are also characterized by tissue degeneration at the site of amyloid deposition. Type II (non insulin-dependent, slow-onset) diabetes is characterized by pancreatic amyloid deposits comprising the 37-amino-acid islet amyloid polypeptide (IAPP, also known as amylin, Fig. 1) [14]. Type II diabetes does not occur in rodents, which may be due to sequence variations between human and rat IAPP that seem to prevent amyloid formation by the rat protein. A synthetic peptide derived from human IAPP (IAPP20–29) forms amyloid fibrils that resemble those formed from full-length IAPP with respect to their ultrastructural dimensions, X-ray diffraction pattern and staining properties [15]. The peptide model of rat IAPP (amino acids 20–29) does not form fibrils, consistent with the behavior of the rat protein [16–19]. As is the case in AD, a causal relationship between amyloid fibril formation and disease has not been established [14].

To rationally design molecules that bind amyloid more tightly than CR or distinguish between amyloid fibrils comprising different proteins, a structure of the amyloid fibril 'receptor' or, even better, of the CR–fibril complex must be determined. The ordered nature of binding is indicated by the fact that amyloid stained with CR exhibits green birefringence when observed using a polarizing light microscope [20]. More detailed structural information is difficult to obtain, since amyloid fibrils are insoluble and noncrystalline [9,10]. Infrared spectroscopy and X-ray diffraction analysis of many amyloid fibrils indicate that they all have a subunit antiparallel β sheet [10]. It has been suggested that this structure represents the CR recognition element, and a crude model of the CR–amyloid complex, characterized by intercalation of CR between the hydrophobic amyloid sheets, has been proposed [20–22]. An alternative electrostatic model for binding of CR to an idealized antiparallel β sheet has been proposed [23,24]. Solid-state NMR studies of β34–42 and IAPP20–29 amyloid fibrils show that, although the β-sheet structures of both amyloids may be unusually compacted, they differ significantly in detail [7,9,10,17,19]. Thus a variety of CR-binding modes may exist. The only detailed structural information regarding a CR–protein complex is a crystal structure of a complex of CR with a soluble, globular insulin dimer [25]. This CR binding mode may not resemble that with an insoluble, non-crystalline amyloid fibril.

In the absence of structural data, a systematic and quantitative structure–activity study of the features of the CR molecule that lead to amyloid binding would be useful. Very little information of this type exists. The binding of CR to two amyloid fibrils, comprising insulin [23,24] or another peptide model of AD brain amyloid (β10–43), has been quantified [26,27]. Furthermore, the affinity of several CR analogs and related aromatic dyes to β10–43 amyloid fibrils has been indirectly measured [26,27]. Based on this information, a crude model of the CR–amyloid complex, featuring electrostatic interactions between the CR sulfonate groups and regularly spaced cationic groups at the amyloid surface has been proposed [26]. This model is not applicable to all amyloid fibrils, as the β34–42 fibril (see below) binds CR but contains no charged side chains.

Here, we describe the relative affinity of a series of CR analogs for two model amyloid fibrils (β34–42 and IAPP20–29) (Figs 1–3 and Table 1). We have chosen to work with peptide models, rather than full-length proteins or naturally-derived material, because the peptides have been extensively characterized, making it possible to eventually describe binding at the molecular level. The results suggest that certain features of CR are important for amyloid fibril binding and reveal that the binding affinity is strongly dependent on the constitution of the amyloid fibril. The latter finding suggests that it may be possible to design small molecule probes that distinguish amyloid fibrils based on their constitution and/or morphology. Such probes may be useful in developing *in vivo* diagnostic agents for diseases characterized by amyloid deposition.

Results and discussion

Synthesis of CR analogs with a modified biphenyl group

A series of CR analogs (Fig. 2, compounds **2–10**) was designed to replace the biphenyl group of CR with related functional groups in which the preferred biphenyl dihedral angle was altered (compounds **2**, **3**, **4**, **6**) or where the

Figure 2

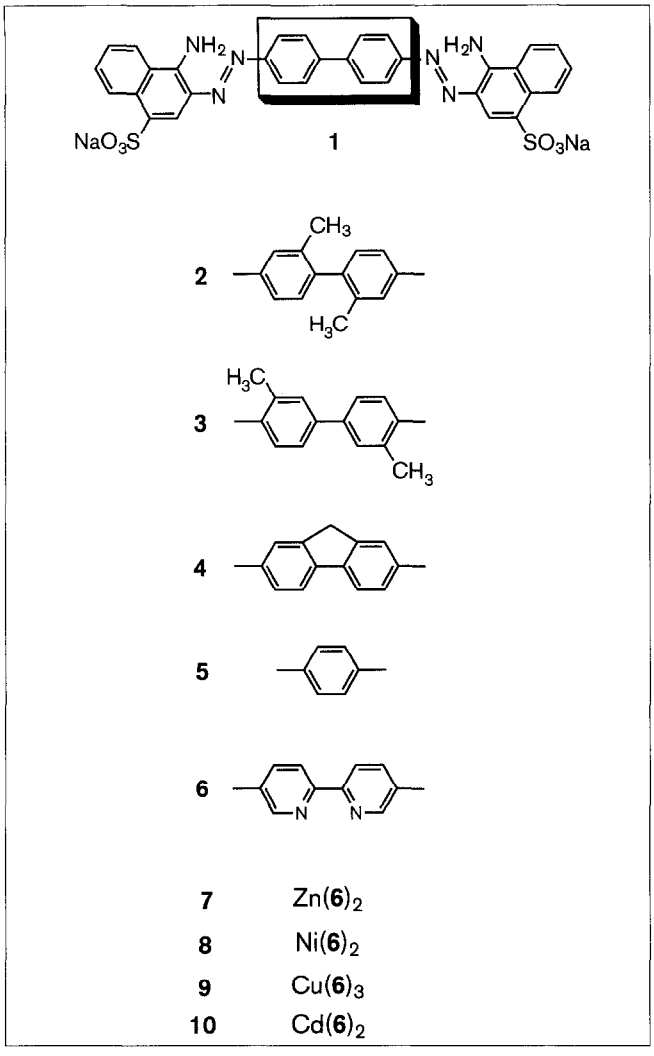

The structures of CR analogs generated by modification of the central biphenyl group (solid box) and chelation of metals by the bipyridyl analog **6**.

naphthyl to naphthyl distance was shortened (compound **5**). Compound **4** is the only one of this group whose synthesis has not been reported previously. These compounds were prepared by a route used for synthesis of CR, replacing the biphenyl 4,4'-diamine intermediate with analogous diamines [28–31]. The commercially available analog 3,3'-dimethyl-CR (benzopurpurin 4B) **3** was intended as a control for 2,2'-dimethyl-CR **2**, as the hydrophobicity of these compounds was expected to be similar. The biphenyl dihedral angle of **3**, however, was expected to be closer to that of CR than the dihedral of compound **2**, which is significantly perturbed relative to CR.

Preparation of metal complexes of the bipyridyl-containing analog 6

To explore the possibility that CR analogs could be used to direct metals to amyloid, which may eventually enable us to image amyloid formation *in vivo*, metal complexation by bipyridyl-CR **6** was investigated (Fig. 2). Metal complexes were prepared by addition of metal salts to aqueous solutions of compound **6**. Complexation was followed and the stoichiometry was determined by UV/visible spectroscopy (Fig. 4). Zinc (complex **7**), nickel (complex **8**), cadmium (complex **10**), and cobalt (not shown) formed complexes with a stoichiometry of one metal ion per two molecules of compound **6** (Fig. 2). Copper formed a complex with a 1:3 stoichiometry (Fig. 2, complex **9**).

Synthesis of CR analogs with modified naphthyl groups

A series of CR analogs were designed to probe the importance of the naphthyl groups for binding to amyloid (Fig. 3, compounds **11–15**). Direct Violet 43 (compound **11**)

Figure 3

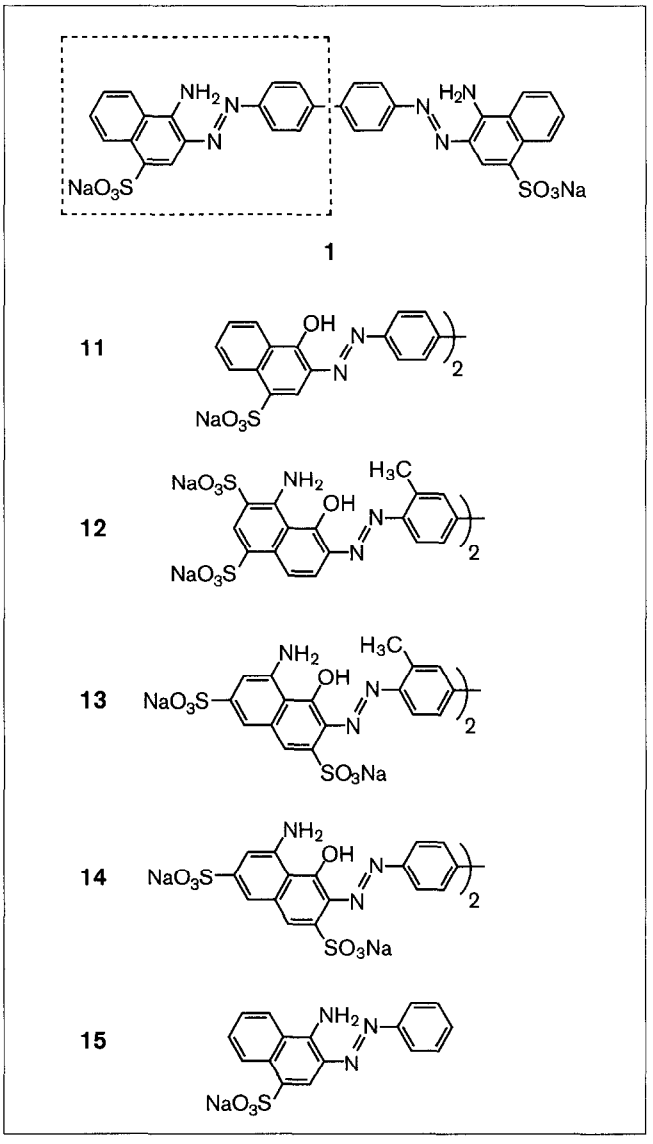

The structures of the CR analogs used in this study generated by modification of the CR terminal naphthyl groups (dotted box).

has the naphthyl amino group replaced by a phenolic hydroxyl group [31]. The commercially available dyes Evans Blue (compound **12**) and Trypan Blue (compound **13**) were also tested, and Direct Blue 6 (compound **14**), an analog of compound **13**, was synthesized [31]. Finally, compound **15**, which represents half of the symmetric CR molecule, was also synthesized [32,33].

CR binds to β34–42 and IAPP20–29 amyloid fibrils with comparable affinity

To conveniently measure the K_d of a given compound directly, a radiolabeled analog of each compound had to be synthesized. Since this was not practical for each analog used in this study, a displacement binding assay was devised in order to measure the relative affinities of each CR analog for the model amyloid fibrils β34–42 and IAPP20–29. ^{35}S-labeled CR was equilibrated with β34–42 or IAPP20–29 amyloid fibrils under conditions where ~85 % of the dye was bound. Increasing concentrations of unlabeled compounds were added, until 50 % of the bound ^{35}S-labeled CR (DC_{50}) was displaced from the fibrils (Fig. 5). For certain compounds, the solubility under the assay conditions was less than the DC_{50}. In these cases, DC_{50} was estimated by extrapolation. The DC_{50} values for CR itself were determined by this method to be 8 (±3) μM for β34–42 and 9 (±3) μM for IAPP20–29 (Table 1). We describe the relative affinities for the two fibrils as a ratio (DC_{50} for IAPP20–29/DC_{50} for β34–42). The affinity ratio for CR is therefore 1.1 (Table 1). This finding is consistent with the fact that CR recognizes a structural feature common to both fibrils. Based on a single experiment,we estimate that the K_d of CR for β34–42 fibrils is 900 nM.

The biphenyl-replacement analogs have a range of affinities for both β34–42 and IAPP20–29 fibrils

None of the purely organic CR analogs bound to the CR binding site of β34–42 or IAPP20–29 amyloid more tightly than CR itself (Table 1). The affinity ratios varied significantly, however. The analogs designed to test the importance of the biphenyl dihedral angle bound slightly less well to both peptide fibrils than did CR, but the flat analog **4** and the orthogonal analog **2** had comparable affinities, suggesting that a slightly twisted biphenyl dihedral angle, present in CR but unreachable by **2** and **4**, may be ideal for binding. The bipyridyl CR analog **6** had comparable affinities to compound **4**, possibly due to its reduced hydrophobicity relative to CR. The affinity of compound **3** for both peptide fibrils was reduced 30- to 70-fold compared to CR, suggesting that hindrance of the naphthyl amine groups by the methyl groups may reduce affinity. The truncated analog **5** had significantly reduced affinity, which may be due to the disposition of the naphthyl binding sites on the fibril [26] or the decreased hydrophobicity of **5** relative to CR. The affinity ratios for this group of analogs varied from 3.7 for compound **2**, which strongly prefers β34–42, to 0.69 for compound **6**, which prefers IAPP20–29.

Metal-bipyridyl-CR complexes bind both amyloids with an affinity comparable to that of CR

Four of the metal complexes of bipyridyl-CR **6** were relatively tight binders to the peptide fibrils, in particular the cadmium complex **10**, which was the only compound analyzed herein which bound more tightly than CR. Complexes **7** and **8** bound IAPP20–29 fibrils more tightly than β34–42 fibrils, whereas complex **10** bound β34–42 fibrils more tightly (Table 1). The cobalt complex of **6** did not bind tightly to either peptide fibril (DC_{50} > 120 μM), possibly due to its aggregation at high concentration. The affinity ratios for the metal complexes ranged from 2.3 for compound **10**, which prefers β34–42, to ~0.6 for compounds

Figure 4

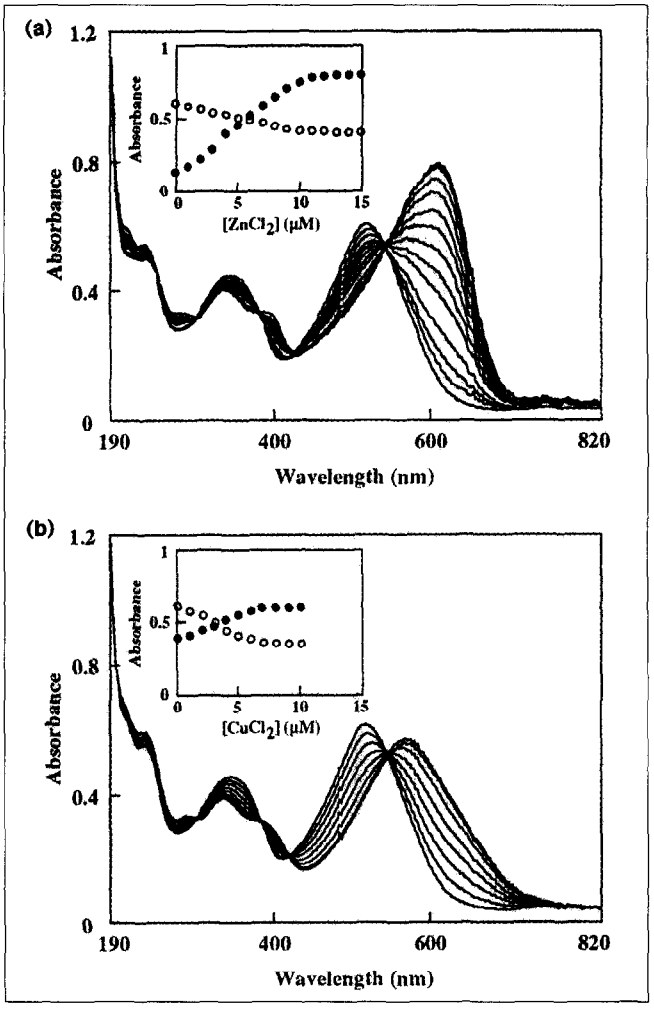

Bipyridyl-CR (compound **6**) binds zinc with a stoichiometry of 2:1 and copper with a stoichiometry of 3:1. The absorption spectra upon titration of compound **6** (21.8 μM) with **(a)** $ZnCl_2$ and **(b)** $CuCl_2$ are shown. Metal ions were added in 1 μM increments. Analyses of the binding isotherm from data taken at 514 nm (○) and 610 nm (●), and at 514 nm (○) and 568 nm(●) are shown in the insert panels in (a) and (b), respectively. The ratios of bipyridyl-CR to $ZnCl_2$ and to $CuCl_2$ are 2:1 and 3:1, respectively.

Figure 5

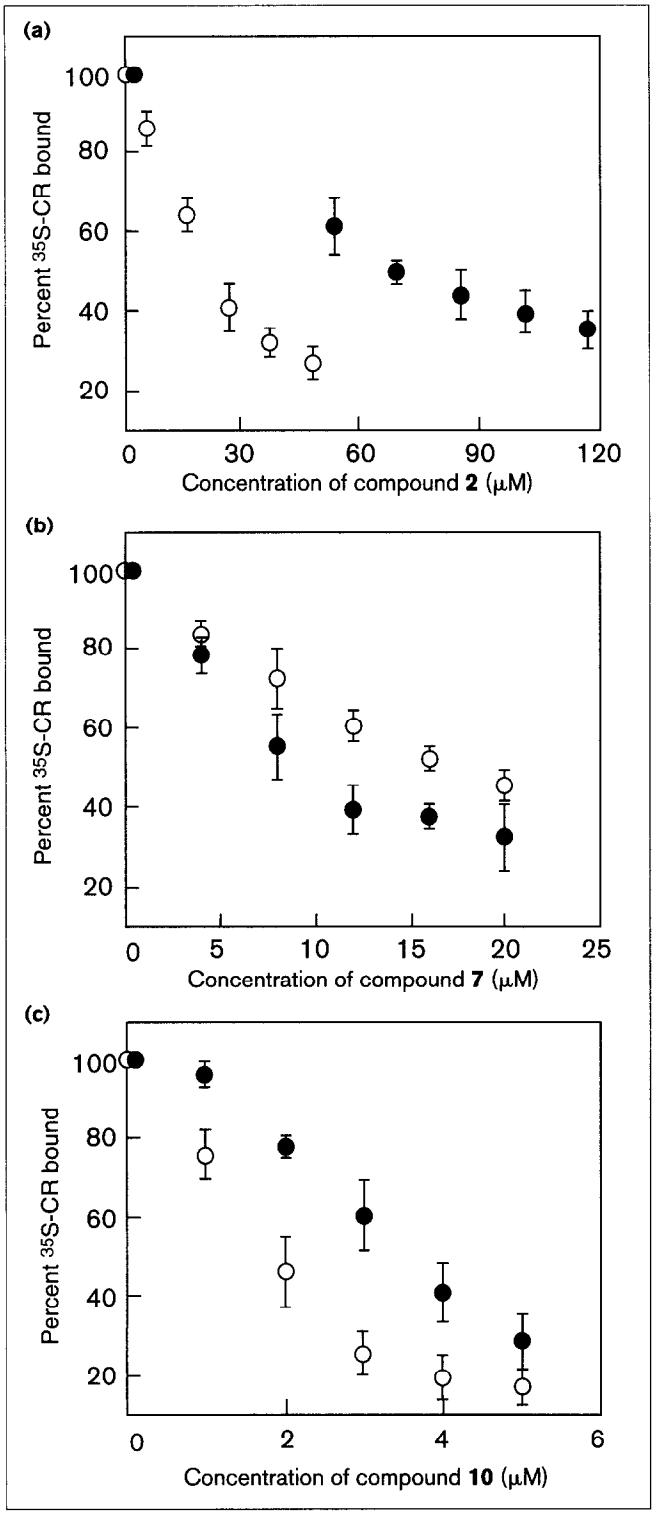

The binding affinities of CR analogs for peptide fibrils as determined by measurement of the displacement of ^{35}S-labeled CR. The displacement profiles for **(a)** 2,2'-dimethyl-CR (compound **2**), **(b)** $Zn(\mathbf{6})_2$ (compound **7**), and **(c)** $Cd(\mathbf{6})_2$ (compound **10**) using 20 μM β34–42 (○) and IAPP20–29 (●) fibrils are shown. The DC_{50} is the concentration of analog required to displace 50 % of the bound CR. Note the difference in the scales of the X axes.

Table 1

DC_{50} values (μM) for displacement of ^{35}S-labeled CR from β34-42 and IAPP20-29 amyloid fibrils with CR and analogs

Compound	β34–42	IAPP20–29	Affinity ratio
1 (CR)	8[c]	9[c]	1.1
2	23[a]	83[a]	3.7
3	229[b]	623[b]	2.8
4	13[a]	20[a]	1.5
5	119[b]	243[c]	2.0
6	19.6[b]	13.5[a]	0.69
7	17.0[b]	9.7[b]	0.57
8	15.8[b]	10.6[b]	0.67
9	20.3[a]	23.0[b]	1.1
10	1.5[b]	3.5[b]	2.3
11	76[c]	93[c]	1.2
12	107[c]	203[a]	1.9
13	62[c]	238[b]	3.8
14	42[b]	123[b]	2.9
15	>4000	>4000	–

Errors (standard deviations) on each of these values were less than [a]10 %, [b]10–20 % or [c]20–40 %. The fourth column reports the ratios of column three to column two, that is, the relative affinities for IAPP20–29 compared to β34–42. A ratio of greater than 1 indicates tighter binding to β34–42, a ratio of less than 1 indicates tighter binding to IAPP20–29. The raw data for compounds **2**, **7** and **10** are presented in Figure 5.

7 and 8, which prefer IAPP20–29. Complex 9, like CR itself, showed little preference. The fact that metal complexes retained their affinity for amyloid inspired the synthesis of a technetium complex of compound 6, which could be useful for SPECT imaging [34].

The naphthyl replacement analogs bind less avidly than CR and with altered selectivity

The CR analogs with modified naphthyl groups bound to both peptide fibrils with lower affinity than CR and most of the biphenyl-replacement analogs. The low affinity of phenolic CR **11** supports the observation that the amine group (see analog **3**) is important in the formation of the CR–amyloid complex. Puchtler *et al.* [2] reported that Trypan Blue (compound **13**) is less effective than CR in staining amyloid fibrils. We confirmed this finding with β34–42 and IAPP20–29 fibrils. Trypan Blue, however, binds to β34–42 fibrils over three-fold more avidly than to fibrils comprising IAPP20–29 (affinity ratio = 3.8). Compound **15** did not displace CR from either fibril (DC_{50} > 4 mM).

Significance

In vivo **amyloid imaging could determine whether amyloid deposition precedes the appearance of symptoms and is, therefore, a possible cause of AD, or whether amyloid deposition follows the appearance of symptoms, being merely a correlated epiphenomenon.**

In the former case, amyloid imaging could be used to diagnose AD. It is also of interest to determine whether the various brain amyloid proteins are deposited in a specific sequence, as would be expected if one particular protein acts as the seed for amyloid fibril formation. A small-molecule probe that, like CR, specifically recognizes the fibrillar amyloid protein and, unlike CR, is specific for one type of amyloid and crosses the blood-brain barrier, would be required for *in vivo* imaging. The studies presented here provide a first step towards development of such a molecule.

The rational design of amyloid probes requires an understanding of the CR–amyloid interaction at the molecular level. Our original goal was to determine the features of the CR molecule that confer affinity for amyloid and to use this information to design more sensitive and specific amyloid probes. The initial assumption that all amyloid fibrils share a common CR-binding site led to the expectation that the effect of a CR modification on amyloid affinity would not depend on the composition of the fibril. The data presented here clearly show that this assumption is not true. Thus, in addition to the general affinity of CR and analogs for all amyloid fibrils, there seems to be some specificity for the particular peptide comprising the fibril. It is thus possible to find CR analogs that distinguish amyloid fibrils of different composition, for example, the brain amyloid proteins β1–40 and NAC. Analogs of this type could be useful in determining the timing of amyloidogenesis by these two proteins in the AD brain.

Finally, an unexpected finding of these studies was that metal binding by a bipyridyl-containing CR analog did not drastically reduce its affinity for amyloid, but altered its affinity ratio for the two amyloids analyzed. This finding suggests the possibility of using metal-CR complexes for the purpose of selective imaging of amyloid deposits.

Materials and methods

General

^{1}H-NMR spectra were recorded with a Varian XL-300 NMR spectrometer (300 MHz) in CD_3OD unless otherwise specified. Chemical shifts are reported in parts per million downfield from tetramethylsilane and coupling constants are reported in Hertz. Mass spectra were recorded using matrix-assisted laser desorption ionization (MALDI) mass spectrometry at the MIT Mass Spectrometry Facility unless otherwise specified. The basic peptide tyrosine protein kinase substrate (TPKS, $[MH]^+ = 1593.74$) was used for MALDI analysis of the CR analogs [35]. Preparative HPLC was performed on a Waters PrepLC 4000 System using a C18 reversed-phase column (30 x 300 mm, 15 μm particle size, 300-Å pore size, YMC, Wilmington, NC) with H_2O and CH_3OH as eluents at a flow rate of 50 ml min^{-1}. Analytical HPLC was performed on a Waters 600E System using a Delta-Pak C18 reversed-phase column (3.9 x 300 mm, 15-μm particle size, 300-Å pore size, Waters, Milford, MA) with H_2O and CH_3OH as eluents at a flow rate of 3 ml min^{-1}. UV spectra were measured on a Hewlett–Packard 8452A diode array spectrophotometer. Extinction coefficients (ε) reported in cm^{-1}•M^{-1} were measured in buffer (10 mM NaH_2PO_4, pH adjusted to 7.4 with 1 N NaOH) unless otherwise specified. CR was purchased from Fluka. 3,3'-Dimethyl-CR (Benzopurpurin 4B), Evans Blue, and Trypan Blue were purchased from Aldrich. These dyes were purified using preparative HPLC before use. 2,2'-Dimethyl-CR (compound **2**) [28,29], phenyl-CR (compound **5**) [30], bipyridyl-CR (compound **6**) [31], Direct Violet 43 (compound **11**) [31], Direct Blue 6 (compound **14**) [31], and truncated CR (compound **15**) [32,33] were synthesized by published procedures. ^{35}S-labeled CR was synthesized as described [36]. β34–42 and IAPP20–29 were prepared by methods reported previously [6,18]. Peptide concentrations were determined by quantitative amino acid analysis.

*General synthetic procedure, applied to 2,2'-dimethyl-CR (compound **2**)*

To a solution of 2,2'-dimethylbenzidine dihydrochloride (199.0 mg, 0.7 mmol) in 10 % HCl (2 ml) at −5 °C was added $NaNO_2$ (106 mg, 1.54 mmol) in H_2O (500 μl). After 5 min, the resulting yellow solution was added dropwise to 4-amino-1-naphthalenesulfonic acid sodium salt (360 mg, 1.47 mmol) and sodium acetate trihydrate (762 mg, 5.6 mmol) in H_2O (6 ml) at −5 °C. A distinct color change was immediately observed. The reaction was allowed to proceed for at least 1 h and the product was purified by preparative HPLC. Typical yields were ~25 %. Purity of the compound was judged to be > 98 % by analytical HPLC and ^{1}H NMR. The other CR derivatives were synthesized using a similar procedure with the appropriate substitution of starting materials [15]. Sodium carbonate replaced sodium acetate for the synthesis of Direct Violet 43 (compound **11**) and Direct Blue 6 (compound **14**). Preparative HPLC; 0–5 min 25 % CH_3OH, 5–20 min 25–100 % CH_3OH. Analytical HPLC; 0–5 min 25 % CH_3OH, 5–20 min 25–100 % CH_3OH, $R_v = 46.5$ ml. ^{1}H NMR δ 8.69 (d, $J = 8.3$, 2H), 8.64 (s, 2H), 8.26 (d, $J = 8.3$, 2H), 7.84 (s, 2H), 7.81 (d, $J = 8.3$, 2H), 7.63 (t, $J = 8.3$, 2H), 7.47 (t, $J = 8.3$, 2H), 7.24 (d, $J = 8.3$, 2H), 2.25 (s, 6H); m/z for $C_{34}H_{28}N_6O_6S_2$, calc'd 680.8, found 680.6; UV λ_{max} 472 ($\epsilon = 1.58 \times 10^4$), 322 ($\epsilon = 2.34 \times 10^4$).

*Fluorenyl-CR (compound **4**)*

Preparative HPLC; 0–5 min 25 % CH_3OH, 5–20 min 25–100 % CH_3OH. Analytical HPLC; 0–5 min 25 % CH_3OH, 5–20 min 25–100 % CH_3OH, $R_v = 49.5$ ml. ^{1}H NMR δ 8.74 (d, $J = 8.4$, 2H), 8.61 (s, 2H), 8.20 (d, $J = 8.4$, 2H), 8.06 (s, 2H), 7.94 (s, 4H), 7.57 (t, $J = 8.4$, 2H), 7.46 (t, $J = 8.4$, 2H), 4.10 (s, 2H); m/z for $C_{33}H_{24}N_6O_6S_2$, calc'd 664.7, found 665.0; UV λ_{max} 498 ($\epsilon = 2.28 \times 10^4$).

*Phenyl-CR (compound **5**)*

Preparative HPLC; 15 % CH_3OH isocratic. Analytical HPLC; 20 % CH_3OH isocratic, $R_v = 10.5$ ml. ^{1}H NMR (DMSO-d_6) δ 8.73 (d, $J = 8.2$, 2H), 8.46 (d, $J = 8.2$, 2H), 8.30 (s, 2H), 8.13 (s, 4H), 7.81 (brs, 4H), 7.59 (t, $J = 8.2$, 2H), 7.49 (t, $J = 8.2$, 2H); m/z for $C_{26}H_{20}N_6O_6S_2$, calc'd 576.6, found 576.2; UV λ_{max} 522 ($\epsilon = 1.64 \times 104$), 336 ($\epsilon = 1.21 \times 10^4$).

*Direct Violet 43 (compound **11**)*

Preparative HPLC; 0–25 min 30–45 % CH_3OH. Analytical HPLC; 0–5 min 25 % CH_3OH, 5–20 min 25–100 % CH_3OH, $R_v = 25.5$ ml. ^{1}H NMR (500 MHz, DMSO-d_6) δ 8.45 (d, $J = 8.5$, 2H), 8.35 (d, $J = 8.5$, 2H), 8.30 (s, 2H), 7.80 (d, $J = 8.5$, 4H), 7.76 (d, $J = 8.5$, 4H), 7.36 (t, $J = 8.5$, 2H), 7.22 (t, $J = 8.5$, 2H); m/z for $C_{32}H_{22}N_4O_8S_2$, calc'd 654.7, found 654.0; UV λ_{max} 538 ($\epsilon = 2.39 \times 10^4$).

*Direct Blue 6 (compound **14**)*

Preparative HPLC; 0–15 min 10–40 % CH_3OH. Analytical HPLC; 0–5 min 5 % CH_3OH, 5–25 min 5–25 % CH_3OH, $R_v = 24.0$ ml. ^{1}H NMR δ 7.71 (d, $J = 8.8$, 4H), 7.64 (d, $J = 8.8$, 4H), 7.50 (s, 2H), 7.12 (d, $J = 1.5$, 2H), 7.10 (d, $J = 1.5$, 2H); m/z for $C_{32}H_{24}N_6O_{14}S_4$, calc'd 844.8, found 844.3; UV λ_{max} 582 ($\epsilon = 4.54 \times 10^4$).

*Truncated CR (compound **15**)*

Preparative HPLC; 0–6 min 15 % CH_3OH, 6–10 min 15–80 % CH_3OH. Analytical HPLC; 10 % CH_3OH isocratic, $R_v = 27$ ml. ^{1}H NMR

(DMSO-d_6) δ 8.72 (d, $J = 9.0$, 1H), 8.44 (d, $J = 9.0$, 1H), 8.28 (s, 1H), 7.96 (d, $J = 7.9$, 2H), 7.72 (s, 2H), 7.61–7.38 (m, 5H); High-resolution MS (positive-ion FAB) for $C_{16}H_{15}N_3O_3S$ $[M + 2H]^+$, calc'd 329.0834, found 329.0830; UV λ_{max} 456 ($\epsilon = 9.9 \times 10^3$), 312 ($\epsilon = 2.0 \times 10^3$).

Measurement of affinity for β34–42 and IAPP20–29 amyloids

Aggregated peptides were prepared by stirring supersaturated solutions of peptide (400 μM) in buffer (100 mM NaH_2PO_4, 0.2 % NaN_3, pH adjusted to 7.4 with 1 N NaOH) for 2 h. To ^{35}S-labeled CR (1 μM) and a varying concentration of the CR analog was added an aggregated peptide solution (50 μl) that remained stirring while aliquots were taken. The solutions were diluted to 1 ml with buffer, briefly vortexed and equilibrated at room temperature for 30 min (20 μM final peptide concentration). Equilibration times greater than 30 min did not show any change in the amount of CR bound. The solutions were then briefly vortexed and filtered through 13 mm extra-thick glass fiber filters (Gelman, Ann Arbor, MI) held in 13 mm 'Pop-Top' filter holders (Nuclepore; Pleasanton, CA). No significant decrease in the concentration of CR was observed after CR solutions were filtered in the absence of fibrils. The amount of ^{35}S-labeled CR bound ([B]) to fibrils was obtained by measuring the radioactivity of the filters and by calculation using the equation $[B] = [T] - [F]$ where [F] is the concentration of ^{35}S-labeled CR in filtrate (i.e., amount unbound or free) and [T] is the total amount of ^{35}S-labeled CR added ($[T] = 1$ μM). The concentration of CR analogs required to competitively decrease the fraction of ^{35}S-labeled CR bound to fibrils by 50 % was defined as the DC_{50} value (Fig. 5). Lower DC_{50} values mean stronger binding and *vice versa*. Each DC_{50} value is an average of at least three separate experiments and each data point in each experiment was performed in triplicate. CR binding was dependent on ionic strength of the solution; the percentage of CR bound to fibrils derived from β34–42 and IAPP20–29 increased with increasing sodium chloride concentration (data not shown).

Determination of metal complex stoichiometries for bipyridyl-CR

The stoichiometry of the metal complexes was determined from titrations performed under saturating conditions ($K_d \ll$ [bipyridyl-CR]) where the stoichiometry of the complex was reflected by the number of equivalents of metal ions needed to reach saturation [37]. Metal titrations were performed in a 1 cm path-length quartz cuvette with bipyridyl-CR solutions (~20 μM) in buffer (10 mM NaH_2PO_4, pH 7.4) at 25 °C. Spectra over the wavelength range 190–820 nm were collected after each addition of metal ions ($ZnCl_2$, $NiCl_2 \cdot 6H_2O$, $CoCl_2 \cdot 6H_2O$, $CuCl_2 \cdot 2H_2O$, or $CdCl_2 \cdot 2.5H_2O$) in 1 μM increments followed by equilibration with stirring for at least 30 min (Fig. 4). Upon addition of metal ions to bipyridyl-CR **6**, the absorptions at 344 and 514 nm decreased in intensity with the concomitant appearance of two new absorptions at ~390 and 610 nm. Bipyridyl-CR:metal stoichiometry determined at λ_{max}; Zn(II) (2:1 ratio, 610 nm, Fig. 4a), Ni(II) (2:1, 592 nm), Cu(II) (3:1, 568 nm, Fig. 4b), Cd(II) (2:1, 606 nm), Co(II) (2:1, 608 nm).

Acknowledgments

We thank the MIT Biopolymers Laboratory for quantitative amino acid analysis. Mass spectral data and interpretation were provided by Andrew Rhomberg of the MIT Mass Spectrometry Facility, which is supported by NIH Grant No. RR00317 (to K. Biemann). This work was supported by the National Institutes of Health (Grant AG08470) and the National Science Foundation (Presidential Young Investigator Award with matching funds from Genentech, Merck and Upjohn). P.T.L. is the Firmenich Associate Professor of Chemistry.

References

1. Selkoe, D.J. (1993). Physiological production of the β-amyloid protein and the mechanism of Alzheimer's disease. *Trends Neurosci.* **16**, 403–409.
2. Puchtler, H., Sweat, F. & Levine, M. (1962). On the binding of Congo Red by amyloid. *J. Histochem. Cytochem.* **10**, 355–364.
3. Khachaturian, Z.S. (1985). Diagnosis of Alzheimer's disease. *Arch. Neurol.* **42**, 1097–1105.
4. Jarrett, J.T., Berger, E.P. & Lansbury, P.T., Jr. (1993). The carboxy terminus of the β amyloid protein is critical for the seeding of amyloid formation: implications for the pathogenesis of Alzheimer's disease. *Biochemistry* **32**, 4693–4697.
5. Iwatsubo, T., Odaka, A., Suzuki, N., Mizusawa, H., Nukina, N. & Ihara, Y. (1994). Visualization of Aβ42(43) and Aβ40 in senile plaques with end-specific Aβ monoclonals: evidence that an initially deposited species is Aβ42(43). *Neuron* **13**, 45–53.
6. Halverson, K., Fraser, P.E., Kirschner, D.A. & Lansbury, P.T., Jr. (1990). Molecular determinants of amyloid deposition in Alzheimer's disease: conformational studies of synthetic β-protein fragments. *Biochemistry* **29**, 2639–2644.
7. Halverson, K.J., Sucholeiki, I., Ashburn, T.T. & Lansbury, P.T., Jr. (1991). Location of β-sheet-forming sequences in amyloid proteins by FTIR. *J. Am. Chem. Soc.* **113**, 6701–6703.
8. Spencer, R.G.S., Halverson, K.J., Auger, M., McDermott, A.E., Griffin, R.G. & Lansbury, P.T., Jr. (1991). An unusual peptide conformation may precipitate amyloid formation in Alzheimer's disease: application of solid-state NMR to the determination of protein secondary structure. *Biochemistry* **30**, 10382–10387.
9. Lansbury, P.T., Jr., *et al.*, & Griffin, R.G. (1995). Structural model for the β-amyloid fibril based on interstrand alignment of an antiparallel-sheet comprising a C-terminal peptide. *Nat. Struct. Biol.* **2**, 990–998.
10. Lansbury, P.T., Jr. (1992). In pursuit of the molecular structure of amyloid plaque: new technology provides unexpected and critical information. *Biochemistry* **31**, 6865–6870.
11. Ueda, K., *et al.*, & Saitoh, T. (1993). Molecular cloning of cDNA encoding an unrecognized component of amyloid in Alzheimer's disease. *Proc. Natl. Acad. Sci. USA* **90**, 11282–11286.
12. Han, H., Weinreb, P.H. & Lansbury, P.T., Jr. (1995). The core Alzheimer's peptide NAC forms amyloid fibrils which seed and are seeded by β-amyloid: is NAC a common trigger or target in neurodegenerative disease? *Chemistry & Biology* **2**, 163–169.
13. Selkoe, D.J. (1995). Deciphering Alzheimer's disease: molecular genetics and cell biology yield major clues. *J. NIH Res.* **7**, 57–64.
14. Nishi, M., Sanke, T., Nagamatsu, S., Bell, G.I. & Steiner, D.F. (1990). Islet amyloid polypeptide: a new β cell secretory product related to islet amyloid deposits. *J. Biol. Chem.* **265**, 4173–4176.
15. Ashburn, T.T. (1995). The molecular basis of pancreatic amyloid deposition in type II diabetes and the binding of Congo Red to amyloid. PhD thesis, Massachusetts Institute of Technology, Cambridge, MA.
16. Glenner, G.G., Eanes, E.D. & Wiley, C.A. (1988). Amyloid fibrils formed from a segment of the pancreatic islet amyloid protein. *Biochem. Biophys. Res. Commun.* **155**, 608–614.
17. Ashburn, T.T., Auger, M. & Lansbury, P.T., Jr. (1992). The structural basis of pancreatic amyloid formation: isotope-edited spectroscopy in the solid state. *J. Am. Chem. Soc.* **114**, 790–791.
18. Ashburn, T.T. & Lansbury, P.T., Jr. (1993). Interspecies sequence variations affect the kinetics and thermodynamics of amyloid formation: peptide models of pancreatic amyloid. *J. Am. Chem. Soc.* **115**, 11012–11013.
19. Griffiths, J.M., Ashburn, T.T., Auger, M., Costa, P.R., Griffin, R.G. & Lansbury, P.T., Jr. (1995). Rotational resonance solid-state NMR elucidates a structural model of pancreatic amyloid. *J. Am. Chem. Soc.* **117**, 3539–3546.
20. Cooper, J.H. (1974). Selective amyloid staining as a function of amyloid composition and structure. *Lab. Invest.* **31**, 232–238.
21. Glenner, G.G., Eanes, E.D. & Page, D.L. (1972). The relation of the properties of Congo Red-stained amyloid fibrils to the β-conformation. *J. Histochem. Cytochem.* **20**, 821–826.
22. Glenner, G.G. (1980). Amyloid deposits and amyloidosis. *New Engl. J. Med.* **302**, 1333–1343.
23. Klunk, W.E., Pettegrew, J.W. & Abraham, D.J. (1989). Quantitative evaluation of Congo Red binding to amyloid-like proteins with a β-pleated sheet conformation. *J. Histochem. Cytochem.* **37**, 1273–1281.
24. Klunk, W.E., Pettegrew, J.W. & Abraham, D.J. (1989). Two simple methods for quantifying low-affinity dye-substrate binding. *J. Histochem. Cytochem.* **37**, 1293–1297.
25. Turnell, W.G. & Finch, J.T. (1992). Binding of the dye Congo Red to the amyloid protein pig insulin reveals a novel homology amongst amyloid-forming peptide sequences. *J. Mol. Biol.* **227**, 1205–1223.
26. Klunk, W.E., Debnath, M.L. & Pettegrew, J.W. (1994). Development of small molecule probes for the β-amyloid protein of Alzheimer's disease. *Neurobiol. Aging* **15**, 691–698.
27. Klunk, W.E., Debnath, M.L. & Pettegrew, J.W. (1995). Chrysamine-G

binding to Alzheimer and control brain: autopsy study of a new amyloid probe. *Neurobiol. Aging* **16**, 541–548.
28. Hori, T., Ott, R.J. & Rys, P. (1980). Sorption and diffusion in ionic dyes in anionic cellophane membranes. *Polym. Eng. Sci.* **20**, 264–270.
29. Hori, T., Ott, R.J. & Rys, P. (1978). Sorption and diffusion of ionic dyes in anionic cellophane membranes. *Org. Coat. Plast. Chem.* **39**, 282–287.
30. Arcoria, A. & Scarlata, G. (1967). Substantivity of azo dyes. I. Disazo compounds from *p*-phenylenediamine, benzidine, 4,4'-diamino-*p*-terphenyl, and diamines with heteroatoms derived from biphenyl. *Ann. Chim.* **57**, 1125–1135.
31. Calogero, F., Freeman, H.S., Esancy, J.F. & Whaley, W.M. (1987). An approach to the design of non-mutagenic azo dyes: 2. Potential replacements for the benzidine moiety of some mutagenic azo dyestuffs. *Dyes Pigm.* **8**, 431–447.
32. Pershin, G.N., Bogdanova, N.S., Znaeva, K.I. & Kraft, M.Y. (1961). Some regularities in influenza virus control with synthetic drugs. *Farmakol. i Toksikol.* **24**, 690–695.
33. Roseira, A.N. & Tolmasquim, E. (1958). The mechanism of color changes in acid solutions of secondary diazo dyes. *Anais Acad. Brasil. Cienc.* **30**, 311–321.
34. Han, H., Cho, C.-G. & Lansbury, P.T., Jr (1996). Technetium complexes for the quantitation of brain amyloid. *J. Am. Chem. Soc.*, in press.
35. Juhasz, P. & Biemann, K. (1994). Mass spectrometric molecular-weight determination of highly acidic compounds of biological significance via their complexes with basic polypeptides. *Proc. Natl. Acad. Sci. USA* **91**, 4333–4337.
36. Knorpp, C.T., Rennie, M.H. & Korst, D.R. (1960). Radiosulfur (S^{35}) labeled Congo Red dye. *J. Nucl. Med.* **1**, 23–30.
37. Tinoco, I., Jr., Sauer, K. & Wang, J.C. (1985). *Physical chemistry: Principles and Applications in Biological Sciences.* (2nd edn), Prentice-Hall, Englewood Cliffs.